Formulation of a Sustained Release Docetaxel Loaded Cockle Shell-Derived Calcium Carbonate Nanoparticles against Breast Cancer

Nahidah Ibrahim Hammadi, Yusuf Abba, Mohd Noor Mohd Hezmee, Intan Shameha Abdul Razak, Alhaji Zubair Jaji, Tijani Isa, et al.

Pharmaceutical Research
An Official Journal of the American Association of Pharmaceutical Scientists

ISSN 0724-8741

Pharm Res
DOI 10.1007/s11095-017-2135-1

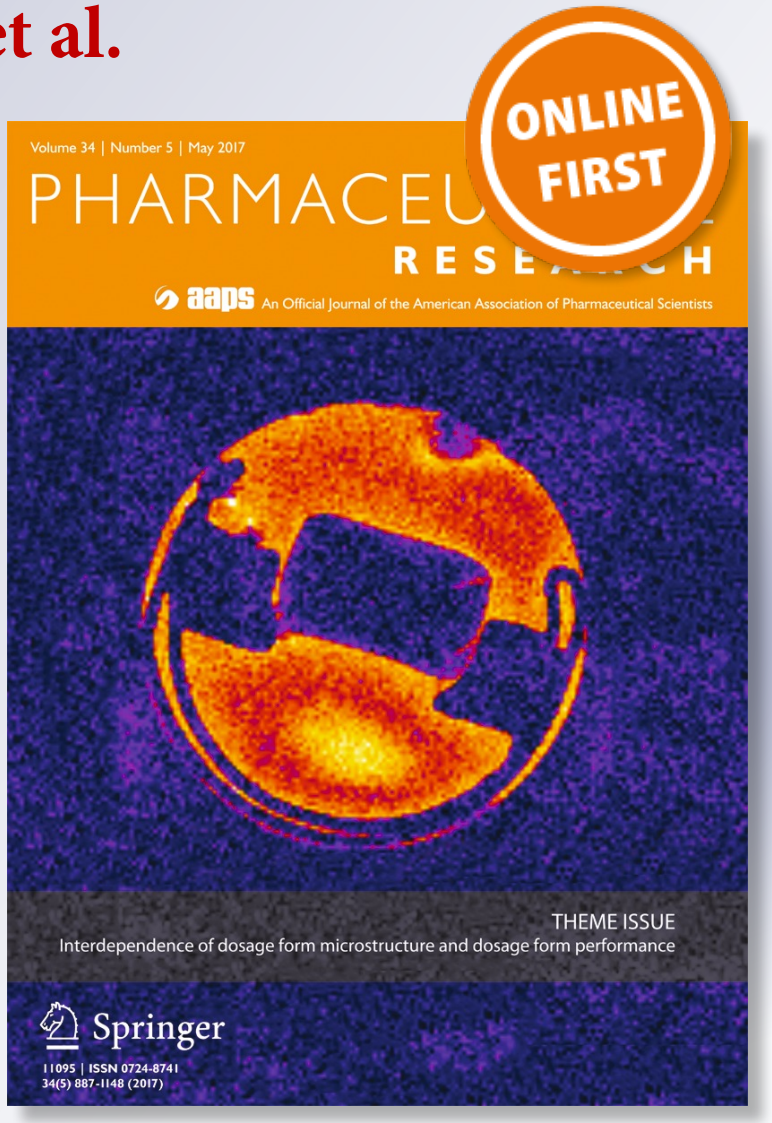

Springer

Pharm Res
DOI 10.1007/s11095-017-2135-1

RESEARCH PAPER

Formulation of a Sustained Release Docetaxel Loaded Cockle Shell-Derived Calcium Carbonate Nanoparticles against Breast Cancer

Nahidah Ibrahim Hammadi[1] • Yusuf Abba[2] • Mohd Noor Mohd Hezmee[1] • Intan Shameha Abdul Razak[1] • Alhaji Zubair Jaji[1] • Tijani Isa[3] • Saffanah Khuder Mahmood[1] • Md Zuki Abu Bakar Zakaria[1]

Received: 6 December 2016 / Accepted: 27 February 2017

ABSTRACT

Purpose Here, we explored the formulation of a calcium carbonate nanoparticle delivery system aimed at enhancing docetaxel (DTX) release in breast cancer.

Methods The designed nano- anticancer formulation was characterized thorough X-ray diffraction (XRD), Fourier transformed infrared (FTIR), transmission electron microscopy (TEM) and field emission scanning electron microscopy (FESEM) and Brunauer-Emmett-Teller (BET) methods. The nano- anticancer formulation (DTX- $CaCO_3$NP) was evaluated for drug delivery properties thorough in vitro release study in human body simulated solution at pH 7.4 and intracellular lysosomal pH 4.8.

Results Characterization revealed the successful synthesis of DTX- $CaCO_3$NP, which had a sustained release at pH 7.4. TEM showed uniformly distributed pleomorphic shaped pure aragonite particles. The highest entrapment efficiency (96%) and loading content (11.5%) were obtained at docetaxel to nanoparticles ratio of 1:4. The XRD patterns revealed strong crystallizations in all the nanoparticles formulation, while FTIR showed chemical interactions between the drug and nanoparticles with negligible positional shift in the peaks before and after DTX loading. BET analysis showed similar isotherms before and after DTX loading. The designed DTX- $CaCO_3$NP had lower ($p < 0.05$) cytotoxity against MCF-7 cells than DTX at 24 h but comparable ($p > 0.05$) effects at 48 h and 72 h. However, the DTX- $CaCO_3$NP released less than 80% of bond DTX at 48 and 72 h but showed comparable effects with free DTX.

Conclusions The results showed that the developed DTX- $CaCO_3$NP released DTX slower at pH 7.4 and had comparable cytotoxicity with free DTX at 48 and 72 h in MCF-7 cells.

KEY WORDS breast cancer · cancer therapy · cockle shell-derived calcium carbonate nanoparticles · drug delivery · nano- anticancer

ABBREVIATIONS

BET	Brunauer-Emmett-Teller
$CaCO_3$	Calcium carbonate
$CaCO_3$NP	Calcium carbonate nanoparticle
DMSO	Dimethylsulfoxide
DTX	Docetaxel
DTX- $CaCO_3$NP	Docetaxel calcium carbonate nanoparticle formulation
EE	Encapsulation efficiency
FESEM	Field emission scanning electron microscopy
FTIR	Fourier transformed infrared
MTT	3-[4, 5- dimethylthiazol-2-yl]-3, 5-diphenyl tetrazolium bromide dye
NP	Nanoparticle
RPMI	Rosewell park memorial institute medium
TEM	Transmission electron microscopy
XRD	X-ray diffraction

Nahidah Ibrahim Hammadi, Yusuf Abba, Mohd Noor Mohd Hezmee, Intan Shameha Abdul Razak, Alhaji Zubair Jaji, Tijani Isa, Saffanah Khuder Mahmood, MD Zuki Abu Bakar Zakaria contributed equally to the manuscript and have read and approved the final manuscript.

✉ Nahidah Ibrahim Hammadi
homamm728@gmail.com

✉ Md Zuki Abu Bakar Zakaria
zuki@upm.edu.my

[1] Department of Veterinary Pre-Clinical Science, Faculty of Veterinary Medicine, Universiti Putra Malaysia, 43400 Serdang, Selangor, Malaysia

[2] Department of Veterinary Pathology and Microbiology Faculty of Veterinary Medicine, Universiti Putra Malaysia, 43400 Serdang, Selangor, Malaysia

[3] Department of Microbiology, Faculty of Science University of Maiduguri, Borno State, Maiduguri, Nigeria

Published online: 05 April 2017

INTRODUCTION

Breast cancer is the number one cause of malignant tumour in women and a major cause of morbidity and mortality among women worldwide. Europe, American and other western countries were shown to have higher incidence of this cancer in the past, however, incidence rates is on the rise in Japan, Singapore, and urban areas of China. These areas were considered traditionally low-incidence region for breast cancer. Changes in life style pattern and reproductive behaviour in these societies were hypothesized to be factors responsible for the demographic shift. The occurrence of breast cancer in men is rare and it is seen in less than 1% of all breast cancer cases (1–3). However, the presentation and diagnosis are usually late perhaps due to poor awareness of the disease occurring in men. The risk of dying death from cancer of the breast in men is relatively lower than in women, though; they are diagnosed with higher stage tumours.

Management of breast cancer is a multidisciplinary task involving chemotherapy, surgery, hormone therapy and radiotherapy mostly in combination. Breast cancer in women diagnosed early has a good prognostic outcome (4), however, effective chemotherapeutic agents are required to reduce the risk of remission after surgery and metastasis (5). Taxanes (paclitaxel or docetaxel) are examples of chemotherapeutic agents that are used to prevent cancer reoccurrence and death in stage 1 cancer patients. However, the major limitation of this compounds is their toxicity to normal body cells (6). Sequestration of the conventional drug system by the reticuloendothelial system, which is composed of monocytes and macrophages, is another major setback faced in cancer treatment. Cumulatively, these factors are responsible for hampering the chemotherapeutic effects of most anti-cancer drugs, necessitating for the development of efficient delivery methods that are less toxic to normal cells (1).

The synthesis, modification and application of nanoparticle are on the increase.; They are used as biosensor, bio imaging, drug delivery vehicle as well as electrical appliances (7, 8). Both organic and inorganic forms of nanoparticles (NP) drug delivery systems have been developed to enhance the intracellular concentration of drugs in solid tumours while avoiding toxicity to normal tissues, utilizing the principle of 'enhanced permeability and retention effect' (EPR effect) (9). The physico- chemical properties of nanoparticles associated with their sizes, shapes and stability makes them an excellent alternative drug delivery vehicle in the management of cancers and other diseases (10). NP showed remarkable distribution into tissues, sustained release ability of the active agent, targeted delivery to particular organs and body tissues and they are generally biocompatible (11).

Calcium carbonate ($CaCO_3$) is one of the most abundant mineral in nature and has three polymorphs; calcite, aragonite and vaterite. Aragonite is a carbonate mineral that naturally occurs in crystal forms as calcium carbonate, aragonite has the same chemistry as calcite but it structure and symmetry is different and it has an orthorhombic crystal structure (12, 13). Biogenic calcium carbonate has come to the attention of many researchers as a promising drug delivery system due to its safety, biodegradability and pH sensitivity (14). Recently, calcium carbonate based nanoparticles, especially the spherically shaped nanoparticles have been utilized as a novel delivery carrier for drugs and bioactive proteins, it shows sustained release and high stability (15, 16). Kamba *et al.* (2013), showed a dose and time dependent effect of a $CaCO_3$NP loaded with doxorubicin on breast cancer cells. The study showed a higher anti-cancer activity of doxorubicin- NP on the breast cancer cells after 72 h of treatment as compared to pure doxorubicin. Doxorubicin release from the $CaCO_3$NP was steady and sustained for days in basic pH than in acidic pH. The cellular uptake mechanism of the NP was shown to be different to that of pure doxorubicin (15).

In this work, we designed a nano-anticancer formulation using cockle shell calcium carbonate nanoparticles ($CaCO_3$NP) loaded with docetaxel (DTX), a hydrophobic anticancer drug. Our primary goal was to evaluate the drug loading capacity, encapsulation efficiency, physico-chemical properties and in vitro release profile of docetaxel- loaded nanoparticles in human body simulated PBS solution at pH 7.4 and PBS solution at pH 4.8. The designed nano-anticancer formulation was further evaluated for therapeutic efficacy against breast cancer (MCF-7) cells in vitro.

MATERIALS AND METHODS

Materials

N-dodecyl-N, N-dimethyl-3-ammonio-1-propanesulfonate BS-12(Sigma-Aldrich 3050 Spruce St. St. Louis, Missouri U.S.A). RPMI 1640 SP Grade for tissue culture (Thermo Fisher Scientific 81 Wyman Street Waltham, MA USA), Ethanol (Joseph Mills Denaturants Liverpool, England), Phosphate Buffer Saline (Sigma-Aldrich 3050 Spruce St. St. Louis, Missouri U.S.A). All other reagents used were of analytical grade and they were used without alteration unless stated otherwise in the experiments.

Synthesis of Calcium Carbonate Nanoparticles

Synthesis of $CaCO_3$NP was done using 5 g of micron-sized cockle shell powders as described previously (16). Briefly, the cockle shell powder was mixed with distilled water and BS-12, stirred for 90 min and filtered. The filtrate was dried in an oven and packaged into a polythene bag and stored for further use (17).

Determination of Drug Loading Efficiency

The preparation of drug loaded $CaCO_3$NP was done according to (13) with a slight modification in the quantity of drug used. Briefly, 25 mg of the $CaCO_3$NP was suspended in 1 mL of distilled deionized water and then made up to a total volume of 10 mL. To this suspension, 2, 4, and 6 mg of DTX dissolved in 1 mL of 0.2% ethanol in deionized water were then added (18). The mixtures were continuously shaken at 200 rpm overnight at room temperature. The resultant particle suspension was centrifuged at 20,000 rpm (4°C) for 15 min and the precipitates were washed thoroughly (15). The amount of free DTX in the solution was used to measure spectrophotometrically at 230 nm. The drug loading content was determined as described previously (15). The absorbance at 230 nm in a UV –vis spectrophotometer were recorded (LAMBDA 25 UV/Vis Systems). Data were given as average measurements of 3 independent values

$$\text{Loading content} = (\text{Wt–Wf})/\text{WnP} \times 100 \quad (1)$$

Where: Wt is the total weight of drug fed, Wf is the weight of non-encapsulated free drug, and Wnp is the weight of the nanoparticle

$$\text{Encapsulation efficiency} = (\text{Wt}-\text{Wf})/\text{Wt} \times 100 \quad (2)$$

Where: Wt is the total weight of drug fed and Wf is the weight of non-encapsulated free drug.

PHYSICO- CHEMICAL CHARACTERIZATION OF NANOPARTICLES AND DRUG LOADING

TEM and FESEM Analysis of DTX-$CaCO_3$NP

The surface morphology and size characterization of the nanoparticles (NP) was performed using a transmission electron microscope (TEM) (Hitachi H-7100, Japan) and a field emission scanning electron microscope, equipped with an energy-dispersive X-ray spectroscopy unit (FESEM/EDX) followed by image analysis using their respective software's respectively. The $CaCO_3$NP and DTX-$CaCO_3$NP were dissolved in 99% ethanol and sonicated for 30 min. One to three drops of each suspension was loaded onto the carbon-covered copper grid and placed on a filter paper to dry at room temperature before viewing with the TEM (16). For the FESEM examination, the samples separately prepared, coated with gold and viewed (19).

Zeta Potential and X-Ray Powder Diffraction

The surface charge and sizes of the NP were measured using Malvern Zetasizer Nano zeta sizer, while the purity and crystalline properties of the $CaCO_3$NP, DTX-$CaCO_3$NP, DTX and $CaCO_3$ were investigated using a Rigaku XRD as described earlier (19).

Fourier-Transform Infrared Spectroscopy

The chemical analyses were done using FT-IR in a range of 280 to 4000 cm^{-1} at a resolution of 2 cm^{-1} and at a scan speed of 64/s. The Pellets of the micron- size $CaCO_3$, $CaCO_3$NP, DTX- $CaCO_3$NP and free DTX powders were mixed individually in a weight proportion of 1 wt% in Kbr powder, and analyses were performed.

In Vitro Drug Release

The in vitro release profiles of DTX from $CaCO_3$NP was determined in PBS (pH 7.4 and pH 4.8) solution according to previous methods with slight modification (1). Two millilitres of PBS containing 2% *v*/v of ethanol was mixed with 10 mg DTX– $CaCO_3$NP and suspended. The tubes were put into an Orbital Shaker incubator (TU-400) at 37°C with a stirring rate of 100 rpm. At scheduled time intervals (0, 15, 30, 45, 60, 75, 90, 105, 120, 135, 150, 165, 180 min), and then at 3, 6, 12, 24, 48, 72, 96, 120 and 200 h), the tubes were taken out and centrifuged at 13, 000 × rpm (Mikro 120, Hettich, Germany) for 15 min. One and a half millilitre of samples were withdrawn and replaced with fresh medium. Docetaxel released from $CaCO_3$NP was evaluated by measuring the optical density at a wavelength λmax =230 nm on Lambda 25 UV/ Spectrophotometer as previously described (20). The results were presented as percentages (%) of drug release against time periods as previously described (15).

In Vitro Cytotoxicity Assay

Cell Culture

Breast cancer cells (MCF-7) were purchased from the American Type Culture Collection (ATCC, Manassas, VA, USA) and cultured in Rosewell Park Memorial Institute medium (RPMI) supplemented with 10% foetal bovine serum, L-glutaminutee (15 mmol/L), penicillin (100 U/mL), and streptomycin (100 靄g/mL). The cells were propagated until 80–90% confluent and then detachment using trypsin, and seeded in a 96-well plate at a density of $1x10^4$ cells/well (21), and incubated at 37°C in a 5% CO_2 incubator for 24 h (22).

MTT Assay

The seeded breast cancer (MCF-7) cells were exposed to different concentrations of DTX, DTX-$CaCO_3$NP, and $CaCO_3$NP in RPMI 1640 medium suspension (0-2 μg/mL), while cells exposed to culture media alone were used as

Table I Drug loading concentration, content, encapsulation efficiency and Zeta potentials ($n = 3$)

Samples	Weight of nanoparticles (mg)	Weight of drug (mg)	Loading content (%)	Encapsulation efficiency (%)
DTX- $CaCO_3$NP1	25	2	3.2	80.1
DTX- $CaCO_3$NP2	25	4	7.1	88.4
DTX- $CaCO_3$NP3	25	6	11.5	96.1

DTX- $CaCO_3$NP; docetaxel- calcium carbonate loaded nanoparticles

control. The NP as well as pure drug were freshly prepared and serially diluted to achieve the required dilutions. After 24, 48, and 72 h incubation with the treatments, 10 µL of 3-[4, 5-dimethylthiazol-2-yl]-3, 5-diphenyl tetrazolium bromide dye (MTT reagent) was added to each well, and the plates were incubated for 4 h at 37°C. The MTT dye was removed and 100 µL of sterile dimethylsulfoxide (DMSO) was added to each well, and shaken in the dark for 30 min to solubilize the crystals and release the colour product into the solution. The experiment was conducted in triplicates, and the optical densities were measured at 570 nm in a micro-titre plate reader (23).

Statistical Analysis

The results obtained were summarized as mean ± SE and analyzed using one-way ANOVA with the Graph pad Prism (Version 6.0) statistical software. Level of significance was set at $p < 0.05$.

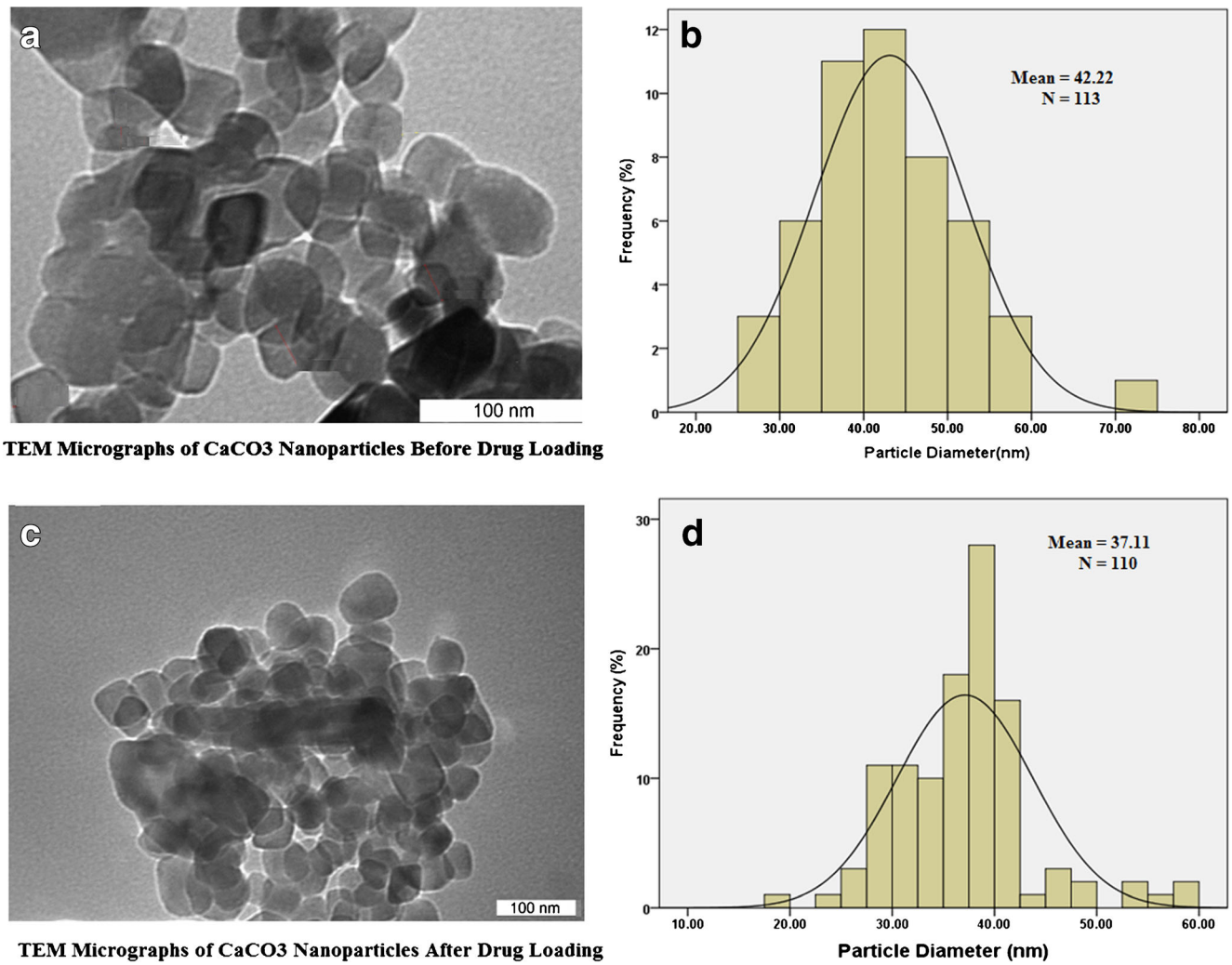

Fig. 1 TEM micrographs showing rounded- shaped calcium carbonate nanoparticles before DTX loading (**a**) and after docetaxel loading (**c**), and the particle size distribution before docetaxel loading (**b**) and after docetaxel loading (**d**).

RESULTS

Docetaxel Loading and Physicochemical Properties of DTX- $CaCO_3$NP

The loading of DTX- $CaCO_3$NP was achieved with different concentration of DTX. The loading contents of DTX-$CaCO_3NP_1$, DTX- $CaCO_3NP_2$, and DTX- $CaCO_3NP_3$ were increased by 3.2%, 7.1%, and 11.5%, with DTX concentrations of 2, 4 and 6 mg/mL, respectively (Table I). Similarly, the encapsulation efficiency (EE) increased from 80.15, 88.45 and 96.1% with increase in the amount of drug. The highest encapsulation efficiency of 96.1% was achieved at a NP: DTX ratio of 1:4.

As shown in (Table I), the efficiency was affected by the amount of drug used and between different drug-nanoparticles ratios. Percentage entrapment of the drug was found to be decreased with decreasing amount of the drug, while an increase in the amount of docetaxel resulted in an increase in the drug entrapment. The surface electrical charge of NP known as the Zeta potential is another important index used in determining the stability of the particle. High absolute value of zeta potential indicates high electric charge on the surface of DTX-$CaCO_3$NP, the higher the charge, the stronger is the repellent forces among particles and the more likely it will prevent aggregation of the NP in solution (24, 25). The Zeta potential of DTX-$CaCO_3$NP was -21.7 ± 0.1 mV, while that of $CaCO_3$NP was -15.4 ± 0.9 and DTX had -8.11 ± 0.7.

The shape of the NP before drug loading was pleomorphic (Fig. 1a). The mean size was found to be 42.22 nm, with a particle size distribution ranging from 25-75 nm (Fig. 1b). The shaped of the drug loaded NP was found similar to the nude NP (Fig. 1c). The mean size of the NP after drug loading was found to be 37.11 nm with a particle size distribution between 18-60n (Fig. 1d).

Figure 2 (a and b) shows the FESEM micrographs of $CaCO_3$NP before and after DTX loading. The morphology of the nanoparticles before and after loading was more or less similar and are fairly rough and pleomorphic in appearance.

XRD and FTIR are usually used as complementary study in nanotechnology to establish the successful synthesis of NP and drug loading, respectively. The XRD spectra (Fig. 3a-c) were those of micron size $CaCO_3$ (Fig. 3a), $CaCO_3$NP (Fig. 3b), DTX (Fig. 3c) and the DTX - $CaCO_3$NP (Fig. 4d). The three spectra shows characteristics peaks of $CaCO_3$ at the 2θ value of 26.5°, 27°, 33.3°, 36.1°, 38.1°, 46.1°, 48.4° and 52°. The peaks were generally sharp and tall in the entire compounds, indicating the persistence of crystallinity in the $CaCO_3$ before and after loading.

The FTIR spectra of DTX, DTX- $CaCO_3$NP and carrier $CaCO_3$NP were shown in Fig. 4 (a, b, c and d, respectively). The FTIR analysis is complementarily with Uv/Vis spectrophotometry results for the successful loading of the drug. The FTIR spectrum of DTX showed bands at 3334.95 cm^{-1} due to O-H and N-H stretching, absorbance at 1447.08 cm^{-1} due to C = C stretching, 1705.83 cm^{-1} spectra due to C = O stretching, and 2979.39 cm^{-1} and 702.34 cm^{-1} spectrum due to C-H stretching. The absorbance spectrum of $CaCO_3$NP alone showed bands at 1455.16 cm^{-1} due to C = C stretching, and 855 cm^{-1} and 708 cm^{-1} due to carbonate (CO_3^{2-}).

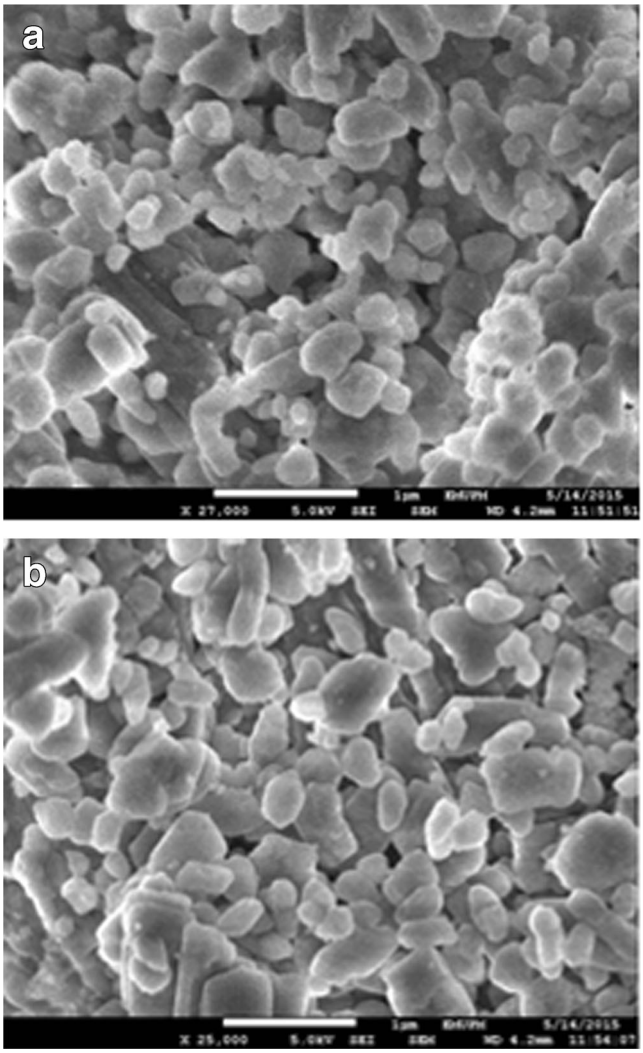

Fig. 2 FESEM micrographs of pleomorphic calcium carbonate nanoparticles before (**a**) and after docetaxel loading (**b**).

As shown in Fig. 5a, the adsorption-desorption isotherm for $CaCO_3$NP is categorized as pore textures. Based on the Brunauer-Emmett-Teller (BET) classification, the compound isotherm is Type III. Figure 5b shows the isotherm of DTX-$CaCO_3$NP, which is similar to the isotherm of the unloaded $CaCO_3$. This indicates that the porous structure of the $CaCO_3$ nanoparticles was still maintained even after DTX loading. As previously shown in the XRD results, the purity of the $CaCO_3$ was still unchanged after loading with DTX.

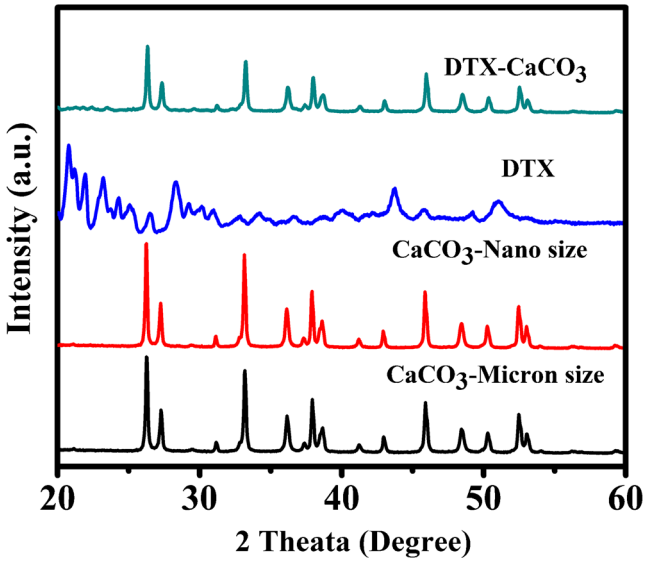

Fig. 3 Powder X-ray diffraction (XRD) patterns of micron size calcium carbonate (**a**), calcium carbonate nanoparticles (**b**), docetaxel (**c**) and docetaxel-calcium carbonate nanoparticles (**d**) showing crystalline phases and purity.

The surface area of both $CaCO_3$NP and DTX-$CaCO_3$NP isotherms as determined by the BET method are shown in Table II.

In Vitro Release Profile of Docetaxel

The readings of the in vitro release profile of DTX from DTX-$CaCO_3$NP were expressed in terms of cumulative percentage of released DTX versus time (Fig. 6). The release study shows three different phases of DTX release at pH 4.8 and 7.4. There is an initial burst, fast and rapid release of about 84% and 45% of the DTX within 3 h at pH 4.8 and 7.4, respectively. Afterwards, there was a continuous slow release of DTX, with 90% released within 6 h at pH 4.8 and approximately 52% of DTX released within the same time at blood physiological pH (7.4). Finally, there was a plateau phase that lasted for three days (72 h), during which about 99% of DTX was released at pH 4.8 and 60% at pH 7.8. The plateau phase at the basic pH continued with a slower release of DTX into the media, cumulating to 95% being released within 200 h (8 days) (Fig. 6).

A burst release seen in both PBS solution of pH 7.4 and 4.8 is likely due to adsorbed docetaxel on the surface of the $CaCO_3$NP. However, the results show that the DTX-$CaCO_3$NP is more stable in an alkaline pH since just 45% of the drug was released from it after 3 h, as in comparison to 84% in the acidic solution.

In Vitro Cytotoxicity Study

The cell viability assay on MCF-7 after treatment with different concentration of $CaCO_3$NP, DTX- $CaCO_3$NP and DTX showed a dose and time dependent effect. Pure DTX and DTX loaded NP demonstrated a progressive decline in the viability of cancer cells. The highest concentration used was 2 μg/mL and the viability of MCF-7 was found to be 55% and 60% after 24 h exposure with pure DTX and DTX loaded NP, respectively. The same concentration of the two compounds (DTX- $CaCO_3$NP and DTX) showed a viability of 22% and 27%, respectively after 72 h exposure. However, even though the DTX treatment alone showed better cancer cytotoxicity at 24 h, it is pertinent to note that less than 80% of the drug bound to the $CaCO_3$NP was released into the medium within this period. Similarly, the amount of drug released at 48 and 72 h were also below 80%, but a similar cytotoxicity with free DTX was observed in the MCF-7 cells.

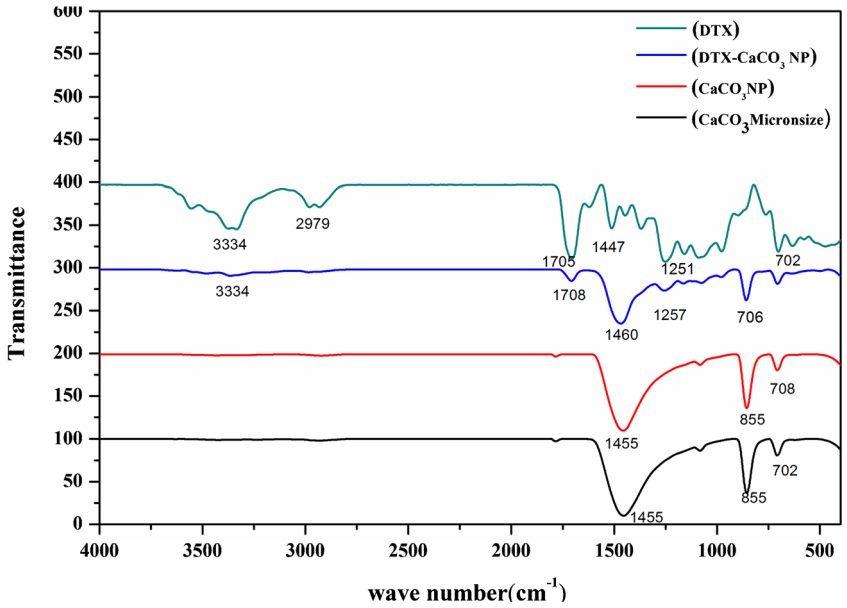

Fig. 4 FTIR spectra of micron size calcium carbonate (**a**), calcium carbonate nanoparticles (**b**), docetaxel- calcium carbonate nanoparticles (**c**) and docetaxel (**d**) depicting the samples absorption or molecular interaction.

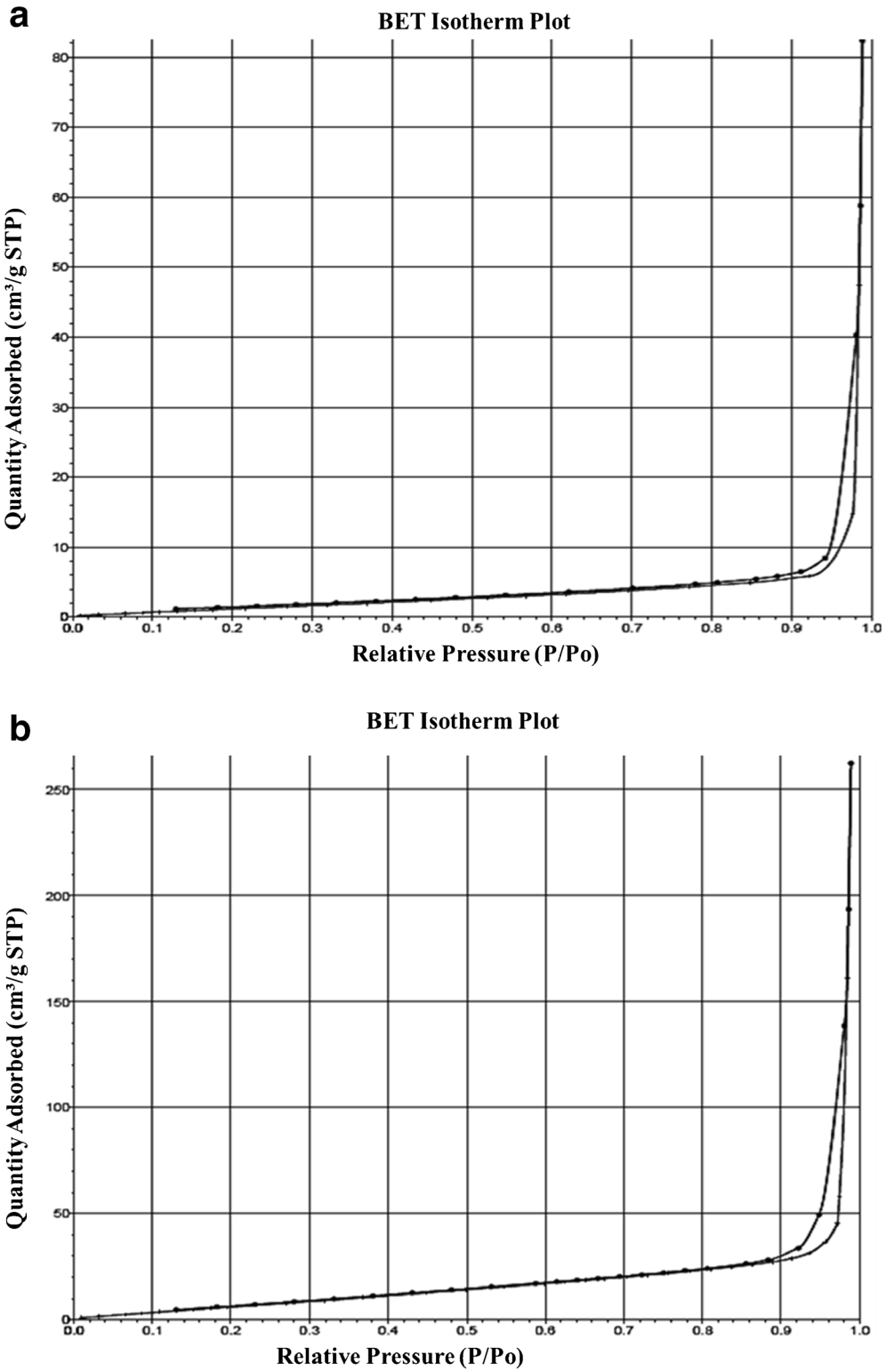

Fig. 5 The diagram shows the adsorption-desorption isotherms for calcium carbonate nanoparticles, the isotherm of the $CaCO_3$NP belongs to Type III based on the IUPAC classification, which refers to it as nano-porous (**a**), and the DTX-$CaCO_3$NP, which has the same isotherm after drug loading (**b**).

This shows that at each concentration, there was a lower dose of DTX released by the $CaCO_3$NP but a comparable effect with free DTX at 48 and 72 h. The $CaCO_3$NP alone showed no toxicity toward the cancer cells even after 72 h exposure at 2 µg/ml concentration (Fig. 7 a, b, c).

The cytotoxicity potential of $CaCO_3$NP alone after 24, 48 and 72 h exposure is shown below (Fig. 8). Different doses were used and the effectiveness was compared to that of pure DTX. However, the concentration of free drug is higher than the concentration of the drug released by the nano carrier at

Table II Surface area, pore volume and pore size of samples

Samples	Surface Area (m^2/g)	Pore volume (cm^3 /g)	Pore size (A°)
$CaCO_3$ NP	6.9529	0.123824	712.3606 Å
DTX-$CaCO_3$NP	38.7340	0.406708	403.6323 Å

24 h. As a result, more concentration of the free drug interacts with the cells than the concentration of the released drug from the nanoparticles that interacts with cells within the initial 24 h treatment period. More of the free drug is therefore endocytosed by the cancer cells than the quantity of free drugs released by the nano carrier. This eventually led to more cell death from cellular interaction with the free drug than the nanoparticles released drug concentrations (µg/mL).

The MCF-7 viability after exposure to $CaCO_3$NP at a concentration as high as 1000 µg/mL showed >86% viability (<15% cytotoxicity) of the cell after 72 h of treatment (Fig. 8). There was more than 90% viability at 500 µg/mL exposure. The slight decrease in cell viability noted with increasing concentrations of $CaCO_3$NP may be attributed to the possible cellular uptake of the NP by the cells.

DISCUSSION

A high percentage of entrapment efficiency of docetaxel in the prepared nanoparticle resulted in minimal loss of drug during the loading process. This may be associated with the surfactant properties exhibited by docetaxel, which played an important role in the size variations of the nanoparticle loaded drug. In our previous studies, we showed that the amount of surfactants used during the preparation process strongly affects the size and morphology of the nanoparticles, which might be liable in preventing particles aggregation complex caused by electrostatic interactions (12, 13, 15). The negative zeta potential of DTX- $CaCO_3$NP was due to the presence of terminal carboxylic groups in the DTX (26). The uptake of negatively charged particles through negative cell membrane of MDA-MB 231 were shown to be via concentration and/or energy dependent manner (27). This suggests that the electrostatic repulsion between the cells and the particles was countered by the NP and energy around the cell membrane.

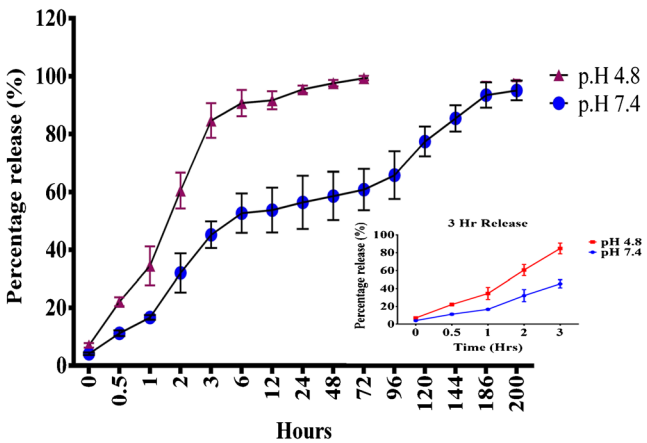

Fig. 6 In vitro docetaxel release profile of calcium carbonate nanoparticles at pH 4.8 and 7.4 over 200 h, the insert shows docetaxel release within 3 h at both pH 4.8 and 7.4. Each bar represents mean ± standard deviation.

The shape, size and surface charges (Zeta potential) of nanoparticles are the characteristic features that influence uptake, distribution, toxicity and targeted drug delivery in various disease treatments. The cellular uptake and delivery of a hexagonal and spherical shaped layered double hydroxide (LDH) nanocomposite into a cell happens via the same endocytic pathway. However, the distributions of the two were shown to be in different regions of the cell. The spherical shaped lodge into the cytoplasm while the hexagonal shaped particle find their way up to the nucleus of the cells (11). In this study, the pleomorphic shaped $CaCO_3$NP had the same morphology after loading with DTX. The newly formed uniformly distributed particles are less than 40 nm in diameter as determined by TEM analysis. Previous studies with other nanomaterials indicated the relationships between the sizes, toxicity, tissue delivery and effectiveness (10). Smaller sizes of less than 5 nm were likely to be taken out of the body system by the kidneys before they rendered their effects, while much larger sizes above 100 nm are more likely to get sequestered by the reticular endothelial system of the spleen and the liver (10). However, the synthesized NP here fall between the two extremes, making them good drug delivery system with less likelihood of being ejected out by the liver, kidney or spleen.

The obtained diffraction spectra of the NP conform to the reference spectra for $CaCO_3$ (JCPDS file no 00–041-1475). Similarly, researcher in the past showed the same pattern of spectra following XRD of $CaCO_3$ that were synthesized by slightly different methods (13, 15, 28). Even though, different drugs were loaded onto the $CaCO_3$NP, the results showed that the crystallinity of the $CaCO_3$NP was maintained after loading, indicating that the method used was repeatable and reliable. Based on the FTIR spectrums, the peaks observed were similar to the reports from earlier studies that utilized $CaCO_3$ as nanocomposites (14, 16, 17) (13). The spectral peaks for DTX-$CaCO_3$NP included peaks from both DTX and $CaCO_3$NP. A spectrum of 3334.2 cm^{-1} was due to functional groups earlier observed in DTX. Similarly, there is a slight shift in spectrum of 708 cm^{-1}, 1460 cm^{-1}, 1257 cm^{-1} and 706 cm^{-1} from earlier observed spectrum of DTX alone. These slight shifts were due to the binding between the drug and the nanoparticle since the $CaCO_3$NP had two similar peaks at 1455 cm^{-1} and 708 cm^{-1}. Thus, the presence of characteristic functional group peaks of DTX and $CaCO_3$NP strongly suggest the successful loading of DTX

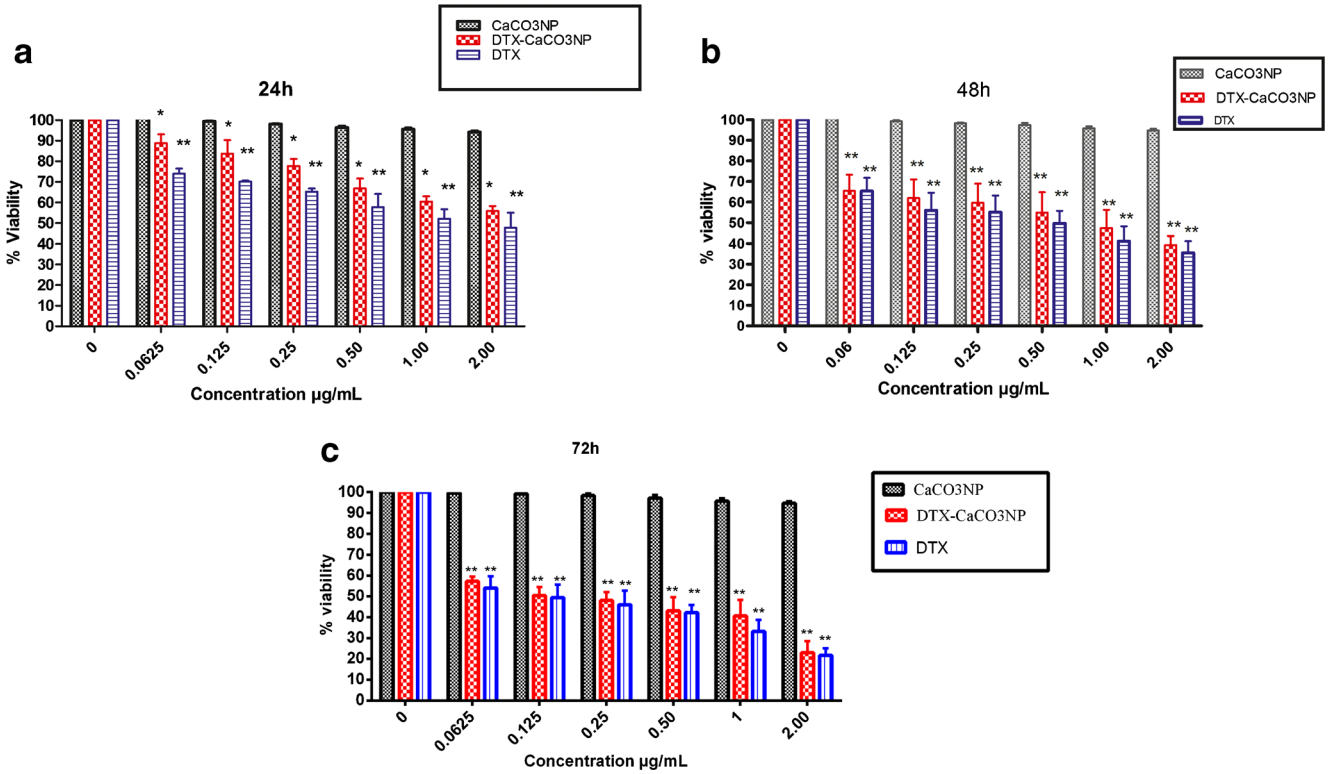

Fig. 7 In vitro cytotoxicity study of MCF-7 cells treated with calcium carbonate nanoparticles, docetaxel- calcium carbonate nanoparticles and docetaxel after 24, 48, and 72 h incubation period. The value represent mean ± standard deviation (=3); * and ** signify significant difference at $p < 0.05$. Bars with different number of asterisk are significantly different.

on to the $CaCO_3$NP. Previous studies utilizing both $CaCO_3$NP and other nano carriers have shown difference in spectral activity after drug loading. Furthermore, the authors also observed retention of most functional groups and in some cases new functional groups after drug loading of the nano carriers (7, 18, 21, 26, 29–31). From the BET results, it can be deduced that an exchange reaction resulted in an increase of the surface area and pore volume of the loaded $CaCO_3$NP, while there was a decrease in pore size after loading. These changes may be possibly due to the DTX loaded both on and inside the $CaCO_3$NP. This may also explain why more drug concentration resulted in more loading as binding of the DTX would have increased the surface area and reduced the pore size of the nanoparticle. Nanoparticle loading of drug is commonly accepted as the sum total amount of bounded drug per polymer mass (32). Loading of drug into a capsular material was suggested as a function of feeding concentration (33). With an increase in DTX feeding concentration, a high loading capacity was observed. At a lower feeding concentration, the loading content became low. The small molecular size of

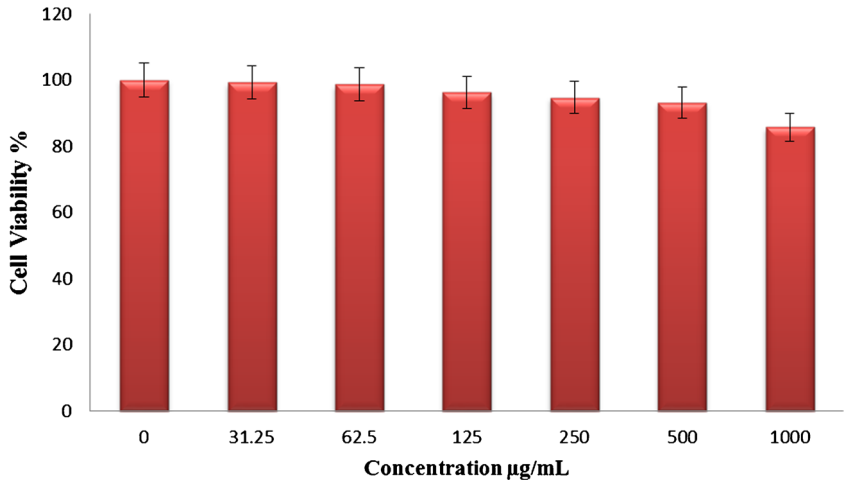

Fig. 8 Cytotoxicity analysis of the blank calcium carbonate nanoparticles on MCF-7 breast cancer cell line.

DTX, and the long overnight loading time was suggested to influence the loading process. Moreover, the increase loading capacity could also be induced by the porous nature of the $CaCO_3$NP.

Our drug release result agrees with earlier studies utilizing different nanodroplets as carriers for DTX. In these studies a peak DTX release was observed after 3 h (31) (1). Sustained release of the anti-cancer drug in the PBS medium of pH 7.4 will enhance bioavailability and decrease dosing frequency. Based on the previous studies, the toxicity of drugs incorporated in nanoparticles is associated with the different mechanisms of the various drugs and hence varies with the drug (8, 15, 27). In addition, collection of previous literature indicated that higher cytotoxicity of drugs formulated into NPs can be attributed to the combination of different but not exclusive mechanisms. The formulated particles will be absorbed through the cell surface resulting in an increased concentration of the drug in the cell membrane, which in turn generates a concentration gradient that aids in the influx of the drug into the cell (1). Drugs like DTX are transported into the cell cytoplasm through a process of passive diffusion. On the other hand, NP are taken up by the cell through endocytosis, which results in an increased cellular uptake of the loaded drug, which enables it to by-pass the effect of ejection from the cell by the P-gp pumps (34). Sánchez-Moreno *et al.* (2012) reported that the sustained release of DTX and its enhanced internalization in MCF-7 cells when in nanocapsule formulation may increase the biological response to DTX and decrease the dose, thereby reducing its adverse effects. Recently another group reported a lower cell viability following treatment of cells with 2 μg/mL of DTX for 2 days, this verifies the sustained release of DTX from the multilayer NPs (31). Drug dose has been a parameter amenable to control. These differences in cytotoxicity are explained by many researchers as result of the mechanism of cellular uptake of the drug. The cellular uptake of free DTX occurs through a passive diffusion mechanism (35), and thereby directly affect the normal cells while in the case of DTX-$CaCO_3$NP, the drug has to be released in a time dependent manner from the $CaCO_3$NP before it exerts its effects on the cells. The mechanism of DTX-$CaCO_3$NP delivery to tumours may circumvent the effect of multidrug resistant proteins which are always present in cancer cells (35). This may thus minimize adverse effects of the drug and thereby facilitate patient compliant behaviour and reduce patient expenses.

The nanoparticle size as well as its zeta potential is the likely cause of cellular uptake of NP as reported with similar inorganic NP usage (28, 29, 36). Thus, $CaCO_3$ as a nano drug carrier system is proven to be biocompatible and non-toxic by itself**.** This finding is in line with previously reported literature (12, 31), which also reported good cyto-compatibility of $CaCO_3$ nanocrystals on MG 63 cells. The cells had a viability of 90% after an exposure concentration of 800–1000 μg/mL of $CaCO_3$ nanocrystals**.** The use of $CaCO_3$ in recent time has gone beyond drug delivery; abundant researches are on-going making this material a leading inorganic materials in biomedical applications (30).

CONCLUSION

In this research we designed a nano-anticancer formulation based on DTX and $CaCO_3$NP. The designed NPs were characterized using XRD, FTIR, TEM, FESEM, UV/Vis and Zeta sizer. The mean size of the $CaCO_3$NP was approximately 42 nm and mean size of DTX- $CaCO_3$NP was approximately 37 nm. The in vitro release of DTX from $CaCO_3$NP was sustained in human body simulated PBS solution of pH 7.4 and pH 4.8. The nano-anticancer formulation showed comparable therapeutic efficacy with free DTX against breast cancer cells even though a lower amount of DTX was released from the $CaCO_3$NP. The results of this research are encouraging to further the studies in animal models for the evaluation of this nano-anticancer formulation. Thus, the research team is currently focusing on the efficacy of the DTX-$CaCO_3$NP on in vivo induced breast cancer in animal models.

ACKNOWLEDGMENTS AND DISCLOSURES

The authors are grateful for funding from Universiti Putra Malaysia Postgraduate Grant Scheme, (GP/ IPS/ 2014/ 9,440,300). The authors declare no conflict of interest.

Data Availability All raw data are available on request from Dr. NIH.

REFERENCES

1. Sanna V, Roggio AM, Posadino AM, Cossu A, Marceddu S, Mariani A, Alzari V, Uzzau S, Pintus G, Sechi M. Novel docetaxel-loaded nanoparticles based on poly (lactide-co-caprolactone) and poly (lactide-co-glycolide-co-caprolactone) for prostate cancer treatment: formulation, characterization, and cytotoxicity studies. Nanoscale Res Lett. 2011;6(1):1–9.
2. Ferlay J, Shin HR, Bray F, Forman D, Mathers C, Parkin DM. Estimates of worldwide burden of cancer in 2008: GLOBOCAN 2008. Int J Cancer. 2010;127(12):2893–917.
3. Sánchez-Moreno P, Boulaiz H, Ortega-Vinuesa JL, Peula-García JM, Aránega A. Novel drug delivery system based on docetaxel-loaded nanocapsules as a therapeutic strategy against breast cancer cells. Int J Mol Sci. 2012;13(4):4906–19.
4. Verma S, Lavasani S, Mackey J, Pritchard K, Clemons M, Dent S, Latreille J, Lemieux J, Provencher L, Verma S. Optimizing the management of HER2-positive early breast cancer: the clinical reality. Curr Oncol. 2010;17(4):20.

5. Group EBCTC. Effects of chemotherapy and hormonal therapy for early breast cancer on recurrence and 15-year survival: an overview of the randomised trials. Lancet. 2005;365(9472):1687–717.
6. Qin Y-Y, Li H, Guo X-J, Ye X-F, Wei X, Zhou Y-H, Zhang X-J, Wang C, Qian W, Lu J. Adjuvant chemotherapy, with or without taxanes, in early or operable breast cancer: a meta-analysis of 19 randomized trials with 30698 patients. PLoS One. 2011;6(11): e26946.
7. Saifullah BaMZH. Inorganic nanolayers: structure, preparation, and biomedical applications. International Journal Journal of nanomedicine IJNM. 2015;10:24.
8. Diaz MR, Vivas-Mejia PE. Nanoparticles as drug delivery Systems in Cancer Medicine: emphasis on RNAi-containing Nanoliposomes. Pharmaceuticals. 2013;6(11):1361–80.
9. Maeda H, Wu J, Sawa T, Matsumura Y, Hori K. Tumor vascular permeability and the EPR effect in macromolecular therapeutics: a review. J Control Release. 2000;65(1):271–84.
10. Kura AU, Hussein MZ, Fakurazi S, Arulselvan P. Layered double hydroxide nanocomposite for drug delivery systems; bio-distribution, toxicity and drug activity enhancement. Chem Cent J. 2014;8(1):1.
11. Kura AU, Saifullah B, Cheah P-S, Hussein MZ, Azmi N, Fakurazi S. Acute oral toxicity and biodistribution study of zinc-aluminium-levodopa nanocomposite. Nanoscale Res Lett. 2015;10(1):1–11.
12. Shafiu Kamba A, Ismail M, Tengku Ibrahim TA, Zakaria ZAB. A pH-sensitive, biobased calcium carbonate aragonite nanocrystal as a novel anticancer delivery system. Biomed Res Int. 2013;2013
13. Kamba AS, Ismail M, Ibrahim TAT, Zakaria ZAB. Synthesis and characterisation of calcium carbonate aragonite nanocrystals from cockle shell powder (Anadara Granosa). J Nanomater. 2013;2013:5.
14. Islam KN, Bakar MZBA, Noordin MM, Hussein MZB, Rahman NSBA, Ali ME. Characterisation of calcium carbonate and its polymorphs from cockle shells (Anadara Granosa). Powder Technol. 2011;213(1):188–91.
15. Kamba SA, Ismail M, Hussein-Al-Ali SH, Ibrahim TAT, Zakaria ZAB. In vitro delivery and controlled release of doxorubicin for targeting osteosarcoma bone cancer. Molecules. 2013;18(9): 10580–98.
16. Islam KN, Bakar MZBA, Ali ME, Hussein MZB, Noordin MM, Loqman M, Miah G, Wahid H, Hashim U. A novel method for the synthesis of calcium carbonate (aragonite) nanoparticles from cockle shells. Powder Technol. 2013;235:70–5.
17. Islam KN, Zuki A, Ali M, Hussein MZB, Noordin M, Loqman M, Wahid H, Hakim M, Hamid SBA. Facile synthesis of calcium carbonate nanoparticles from cockle shells. J Nanomater. 2012;2012:2.
18. Fang G, Tang B, Liu Z, Gou J, Zhang Y, Xu H, Tang X. Novel hydrophobin-coated docetaxel nanoparticles for intravenous delivery: in vitro characteristics and in vivo performance. Eur J Pharm Sci. 2014;60:1–9.
19. Isa T, Zakaria ZAB, Rukayadi Y, Mohd Hezmee MN, Jaji AZ, Imam MU, Hammadi NI, Mahmood SK. Antibacterial activity of ciprofloxacin-encapsulated cockle shells calcium carbonate (aragonite) nanoparticles and its biocompatability in macrophage J774A. Int J Mol Sci. 2016;17(5):713.
20. Sheetal M. A simple ultraviolet spectrophotometric method for the estimation of docetaxel in bulk drug and formulation. A J Pharm Anal. 2013;3(2):48–52.
21. Kim BJ, Min KH, Hwang GH, Lee HJ, Jeong SY, Kim E-C, Lee SC. Calcium carbonate-mineralized polymer nanoparticles for pH-responsive robust nanocarriers of docetaxel. Macromol Res. 2015;23(1):111–7.
22. Trebuňová M, Laputková G, Géci I, Andrašina I, Sabo J. Enhancement of docetaxel-treated MCF-7 cell death by 900-MHz radiation. Cent Eur J Biol. 2013;8(4):357–65.
23. Shafiu KA, Ismail M, Tengku Ibrahim TA, ZAB Z, Hassan Gusau L. In Vitro Ultrastructural Changes of MCF-7 for Metastasise Bone Cancer and Induction of Apoptosis via Mitochondrial Cytochrome C Released by CaCO 3/Dox Nanocrystals. Biomed Res Int. 2014;2014
24. Miller ML, Andringa A, Dixon K, Carty MP. Insights into UV-induced apoptosis: ultrastructure, trichrome stain and spectral imaging. Micron. 2002;33(2):157–66.
25. Nagda C, Chotai N, Patel S, Soni T, Patel U. Preparation and in vitro evaluation of bioadhesive microparticulate system. Intern J Pharm Sci Nanotechnol. 2008;1(3):257–66.
26. Feng L, Wu H, Ma P, Mumper RJ, Benhabbour SR. Development and optimization of oil-filled lipid nanoparticles containing docetaxel conjugates designed to control the drug release rate in vitro and in vivo. Int J Nanomedicine. 2011;6:2545.
27. Youm I, Bazzil JD, Otto JW, Caruso AN, Murowchick JB, Youan B-BC. Influence of surface chemistry on cytotoxicity and cellular uptake of nanocapsules in breast cancer and phagocytic cells. AAPS J. 2014;16(3):550–67.
28. Saidykhan L, Bakar MZBA, Rukayadi Y, Kura AU, Latifah SY. Development of nanoantibiotic delivery system using cockle shell-derived aragonite nanoparticles for treatment of osteomyelitis. Int J Nanomedicine. 2016;11:661.
29. Xu ZP, Zeng QH, Lu GQ, Yu AB. Inorganic nanoparticles as carriers for efficient cellular delivery. Chem Eng Sci. 2006;61(3): 1027–40.
30. Wang J, Chen J-S, Zong J-Y, Zhao D, Li F, Zhuo R-X, Cheng S-X. Calcium carbonate/carboxymethyl chitosan hybrid microspheres and nanospheres for drug delivery. J Phys Chem C. 2010;114(44): 18940–5.
31. Oh KS, Kim K, Yoon BD, Lee HJ, Park DY, Kim E-y, Lee K, Seo JH, Yuk SH. Docetaxel-loaded multilayer nanoparticles with nanodroplets for cancer therapy. Int J Nanomedicine. 2016;11: 1077.
32. Das S, Banerjee R, Bellare J. Aspirin loaded albumin nanoparticles by coacervation: implications in drug delivery. Trends Biomater Artif Organs. 2005;18(2):203–12.
33. Mao Z, Ma L, Gao C, Shen J. Preformed microcapsules for loading and sustained release of ciprofloxacin hydrochloride. J Control Release. 2005;104(1):193–202.
34. Li Y, Jin M, Shao S, Huang W, Yang F, Chen W, Zhang S, Xia G, Gao Z. Small-sized polymeric micelles incorporating docetaxel suppress distant metastases in the clinically-relevant 4T1 mouse breast cancer model. BMC Cancer. 2014;14(1):329.
35. Singh SK, Banala VT, Gupta GK, Verma A, Shukla R, Pawar VK, Tripathi P, Mishra PR. Development of docetaxel nanocapsules for improving in vitro cytotoxicity and cellular uptake in MCF-7 cells. Drug Dev Ind Pharm. 2015;41(11):1759–68.
36. Wang T, Petrenko VA, Torchilin VP. Paclitaxel-loaded polymeric micelles modified with MCF-7 cell-specific phage protein: enhanced binding to target cancer cells and increased cytotoxicity. Mol Pharm. 2010;7(4):1007–14.